

# Femtosecond synchronously in-well pumped vertical-external-cavity surface-emitting laser

Wei Zhang<sup>1,\*</sup>, Alison McDonald<sup>1</sup>, Thorsten Ackemann<sup>2</sup>, Erling Riis<sup>2</sup>, Gail McConnell<sup>1</sup>

<sup>1</sup>Centre for Biophotonics, SIPBS, University of Strathclyde, Glasgow, G4 0NR, UK

<sup>2</sup>SUPA, Department of Physics, University of Strathclyde, Glasgow, G4 0NG, UK

\*wei.zhang.100@strath.ac.uk

**Abstract:** We demonstrate the first synchronously in-well pumped vertical-external-cavity surface-emitting laser (VECSEL). Depending on the cavity mismatch, laser pulses with a duration from 1 ps to 7 ps at a repetition rate of 76 MHz were generated directly from the laser at 860 nm. The application of extra-cavity pulse compression further shortened the pulse to a duration of 210 fs providing a peak power of 226 W.

©2009 Optical Society of America

**OCIS codes:** (040.4200) Multiple quantum wells; (140.5960) Semiconductor lasers; (320.1590) Chirping; (320.5520) Pulse compression.

---

## References and links

1. A. C. Tropper, H. D. Foreman, A. Garnache, K. G. Wilcox, and S. H. Hoogland, "Vertical-external-cavity semiconductor lasers," *J. Phys. D Appl. Phys.* **37**(9), R75–R85 (2004).
2. U. Keller, K. J. Weingarten, F. X. Kärtner, D. Kopf, B. Braun, I. D. Jung, R. Fluck, C. Hönninger, N. Matuschek, and J. Aus der Au, "Semiconductor saturable absorber mirrors (SESAMs) for femtosecond to nanosecond pulse generation in solid-state lasers," *IEEE J. Sel. Top. Quantum Electron.* **2**(3), 435–453 (1996).
3. K. G. Wilcox, Z. Mihoubi, G. J. Daniell, S. Elsmere, A. Quarterman, I. Farrer, D. A. Ritchie, and A. Tropper, "Ultrafast optical Stark mode-locked semiconductor laser," *Opt. Lett.* **33**(23), 2797–2799 (2008).
4. D. Lorenser, D. J. H. C. Maas, H. J. Unold, A. R. Bellancourt, B. Rudin, E. Gini, D. Ebling, and U. Keller, "50-GHz passively mode-locked surface-emitting semiconductor laser with 100 mW average output power," *IEEE J. Quantum Electron.* **42**(8), 838–847 (2006).
5. A. Aschwanden, D. Lorenser, H. J. Unold, R. Paschotta, E. Gini, and U. Keller, "2.1-W picosecond passively mode-locked external-cavity semiconductor laser," *Opt. Lett.* **30**(3), 272–274 (2005).
6. W. Denk, J. H. Strickler, and W. W. Webb, "Two-photon laser scanning fluorescence microscopy," *Science* **248**(4951), 73–76 (1990).
7. A. Zumbusch, G. R. Holtom, and X. S. Xie, "Three-dimensional vibrational imaging by coherent anti-Stokes Raman scattering," *Phys. Rev. Lett.* **82**(20), 4142–4145 (1999).
8. W. B. Jiang, R. Mirin, and J. E. Bowers, "Mode-locked GaAs vertical cavity surface emitting lasers," *Appl. Phys. Lett.* **60**(6), 677–679 (1992).
9. W. B. Jiang, S. R. Friberg, H. Iwamura, and Y. Yamamoto, "High powers and subpicosecond pulses from an external-cavity surface-emitting InGaAs/InP multiple quantum well laser," *Appl. Phys. Lett.* **58**(8), 807–809 (1991).
10. W. H. Xiang, S. R. Friberg, K. Watanabe, S. Machida, W. B. Jiang, H. Iwamura, and Y. Yamamoto, "Femtosecond external-cavity surface-emitting InGaAs/InP multiple-quantum-well laser," *Opt. Lett.* **16**(18), 1394–1396 (1991).
11. W. Zhang, T. Ackemann, M. Schmid, N. Langford, and A. I. Ferguson, "Femtosecond synchronously mode-locked vertical-external-cavity surface-emitting laser," *Opt. Express* **14**(5), 1810–1821 (2006).
12. W. B. Jiang, D. J. Derickson, and J. E. Bowers, "Analysis of laser pulse chirping in mode-locked vertical-cavity surface-emitting lasers," *IEEE J. Quantum Electron.* **29**(5), 1309–1318 (1993).
13. A. R. Zakharian, J. Hader, J. V. Moloney, S. W. Koch, P. Brick, and S. Lutgen, "Experimental and theoretical analysis of optically pumped semiconductor disk lasers," *Appl. Phys. Lett.* **83**(7), 1313–1315 (2003).
14. M. Kolesik, and J. V. Moloney, "Time-Domain Vertical-External-Cavity Semiconductor Laser Simulation," *IEEE J. Quantum Electron.* **43**(7), 588–596 (2007).
15. W. Zhang, T. Ackemann, S. J. McGinily, M. Schmid, E. Riis, and A. I. Ferguson, "Operation of an optical in-well-pumped vertical-external-cavity surface-emitting laser," *Appl. Opt.* **45**(29), 7729–7735 (2006).
16. M. Schmid, S. Benhabane, F. Torabi-Goudarzi, R. Abram, A. I. Ferguson, and E. Riis, "Optical in-well pumping of a vertical-external-cavity surface-emitting laser," *Appl. Phys. Lett.* **84**(24), 4860–4862 (2004).
17. M. Y. A. Raja, S. R. J. Brueck, M. Osinsky, C. F. Schaus, J. G. McInerney, T. M. Brennan, and B. E. Hammons, "Resonant periodic gain surface-emitting semiconductor lasers," *IEEE J. Quantum Electron.* **25**(6), 1500–1512 (1989).
18. S. W. Corzing, R. S. Geels, J. W. Scott, R. H. Yan, and L. A. Coldren, "Design of Fabry-Perot surface-emitting lasers with a periodic gain structure," *IEEE J. Quantum Electron.* **25**(6), 1513–1524 (1989).

19. S. J. McGinily, R. H. Abram, K. S. Gardner, E. Riis, A. I. Ferguson, and J. S. Roberts, "Novel gain medium design for short-wavelength vertical-external-cavity surface-emitting laser," *IEEE J. Quantum Electron.* **43**(6), 445–450 (2007).
  20. C. P. Ausschnitt, R. K. Jain, and J. P. Heritage, "Cavity length detuning characteristics of the synchronously mode-locked CW dye laser," *IEEE J. Quantum Electron.* **15**(9), 912–917 (1979).
  21. U. Morgner, and F. Mitschke, "Drift instabilities in the pulses from cw mode-locked lasers," *Phys. Rev. E Stat. Phys. Plasmas Fluids Relat. Interdiscip. Topics* **58**(1), 187–192 (1998).
  22. C. H. Henry, "Theory of the linewidth of semiconductor lasers," *IEEE J. Quantum Electron.* **18**(2), 259–264 (1982).
  23. G. P. A. Malcolm, and A. I. Ferguson, "Synchronously pumped continuous-wave dye laser pumped by a mode-locked frequency-doubled diode-pumped Nd:YLF laser," *Opt. Lett.* **16**(11), 814–816 (1991).
  24. G. McConnell, and E. Riis, "Ultra-short pulse compression using photonic crystal fibre," *Appl. Phys. B* **78**(5), 557–563 (2004).
- 

## 1. Introduction

Vertical-external-cavity surface-emitting lasers (VECSELs) have been demonstrated to produce high continuous wave (CW) average output powers with excellent beam quality [1]. These are mainly optically pumped multiple quantum well (MQW) based semiconductor lasers offering flexibility in lasing and pump wavelengths arising from band-gap engineering. The external cavity geometry is controlling the spatial and longitudinal mode properties of the output. It provides the possibility of inserting e.g. birefringent or dispersive elements into the cavity as well as allowing an independent and accurate control of the cavity length. In addition, a broad gain bandwidth makes VECSELs an attractive source for ultra-short pulse generation. To date, most successful experiments have focused on passive mode locking using a semiconductor saturable absorber mirror (SESAM) [2] resulting in the generation of sub-500 fs pulses [3] at high repetition rates [4] with high average output powers [5]. These devices operate in a regime commensurate with the requirements of optical communications systems. However, the short energy storage time in the semiconductor gain medium favors the high repetition rates achieved and results in a relatively modest peak power of the individual pulse of order up to ~100 W [3, 5]. This makes them unsuitable for biological imaging applications, e.g. two photon microscopy [6] and coherent anti-Stokes Raman scattering (CARS) microscopy [7], where higher peak power pulses are required to increase the efficiency of the nonlinear optical processes. Indeed, operation at low repetition rates (10-100 MHz) is actually preferable to due to the lifetimes of the fluorescent markers typically used in biological imaging.

Synchronously pumped mode-locking of a VECSEL offers the potential for producing high peak power pulses at a repetition rate in the tens to hundreds of MHz range. Previous studies [8–11] have demonstrated femtosecond pulses with kW peak powers (after extra-cavity pulse compression). The temporal profiles of the pulses directly generated from the lasers are generally tens of picoseconds wide with a strong chirp originating from self phase modulation (SPM) in the laser amplifier due to optical pumping and gain saturation [12]. It should, however, be noted that all of these early studies are based on the standard VECSEL pumping technique of exciting carriers in the relatively wide barrier layers between the quantum wells. These systems are characterized by a large amount of chirp while the carrier capture time of ~20 ps [13, 14] limits the speed of gain dynamics. For an optical in-well pumped system [15, 16], where the carriers are generated directly in the QWs, the carrier transportation time is eliminated. The faster build-up of the gain will affect the pulse shape and potentially lead to a reduction of the chirp. Furthermore, in-well pumping increases the range of pump sources suitable for a specific VECSEL wavelength. For example, barrier pumping of 850 nm lasers typically requires a mode-locked pump source with a wavelength shorter than 700 nm. This spectral range is primarily served by the technically demanding colliding pulse dye lasers.

In this paper, we report the first operation of a synchronously in-well pumped VECSEL. The laser produced a maximum output power of 11.8 mW at ~865 nm. Depending on the amount of the cavity length mismatch, 1 ps to 7 ps pulses were generated directly by the laser oscillator. Effective pulse compression was achieved by using either a photonic crystal fiber

(PCF) or a standard telecommunication fiber. Pulses as short as 210 fs were obtained with a peak power of 226 W.

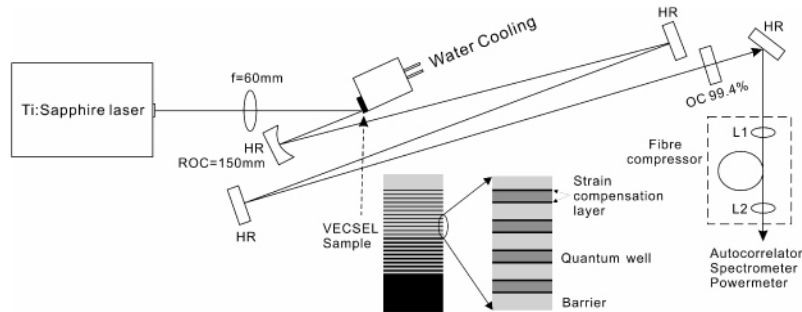


Fig. 1. , Schematic setup of the synchronously pumped VECSEL; output pulses were observed either directly or after compression by a PCF or a telecom fiber; the fiber coupling lenses L1 and L2 were anti-reflection coated aspheric lenses; for the PCF based compressor, L1,  $f=3.3$  mm and  $NA=0.68$  and L2,  $f=2.75$  mm and  $NA=0.65$ ; for the telecom fiber based compressor, L1,  $f=6.24$  mm and  $NA=0.4$  and L2,  $f=2.75$  mm and  $NA=0.65$ . Details of the MQW gain structure are given in the text.

## 2. Experimental setup

The schematic structure of the VECSEL gain element and the laser cavity are shown in Fig. 1. The VECSEL wafer used in this work was grown by MOCVD. It was originally designed for conventional barrier pumping. A semiconductor Bragg mirror was first deposited on top of a GaAs wafer. This high-reflectivity (HR) mirror has its central wavelength at 850 nm for normal incidence and a bandwidth of 85 nm FWHM. Above the mirror is a 17 QW strain compensated gain structure with a peak emission at 850 nm. The 10 nm wide wells are separated by approximately half a wavelength of AlGaAs. A further layer of AlGaAs is added on top of the gain structure to increase the total length of the micro-cavity to 2.55  $\mu\text{m}$ . This corresponds to an anti-resonant structure at 850 nm. Compared with a resonant gain structure [17, 18], the anti-resonant design minimizes spectral filtering and thus provides a larger gain bandwidth beneficial for wavelength tuning and generation of ultra-short pulses through mode-locking. Finally, a 20 nm layer of GaAsP was added to prevent oxidation. A detailed discussion and characterization of the material is reported by McGinily *et al.* [19]. The band-gap of the AlGaAs barriers is 1.748 eV corresponding to a wavelength of 710 nm so wavelengths longer than this are only absorbed by the quantum wells. Due to the correspondingly smaller volume of absorbing material the absorption is significantly reduced. It is therefore desirable to choose an in-well pumping wavelength that is sufficiently long to be reflected by the Bragg mirror and sent through the MQW region a second time (or potentially recycled several times with a more sophisticated pumping scheme).

A 3 mm  $\times$  3 mm sized VECSEL sample was cleaved from the wafer and then bonded to a water-cooled copper block by using indium foil. The whole copper block was maintained at a stable temperature of 1.7  $^{\circ}\text{C}$ . The back surface of the sample was roughened to minimize the etalon effect of the substrate layer. The laser cavity consisted of the HR Bragg mirror, a HR curved mirror with 150 mm radius of curvature, two plane HR mirrors and a wedged output coupling mirror with a reflectivity of 99.4% at 850 nm. The output coupler was mounted on a translation stage providing fine cavity length adjustment. The external cavity was designed to have a mode size of 20  $\mu\text{m}$  in radius on the sample and the total cavity length was designed to match the cavity length of the pump laser. The 140 fs pump pulses at a repetition rate of 76 MHz were generated by a commercial Ti:Sapphire laser (Mira 900F, Coherent Inc.). The pump pulses were focused into the gain medium by a lens with a focus length of 60 mm to match the pump mode to the laser cavity mode. The maximum pump power at the VECSEL gain medium was about 480 mW in the 800 nm wavelength region.

### 3. Experimental results

The VECSEL was synchronously mode-locked by matching the external cavity length to that of the pump laser. The maximum output power was obtained at a pump wavelength of 793 nm where the reflected pump power was measured to be 200 mW. Hence 280 mW was absorbed. The corresponding output power was 11.8 mW. Threshold was reached at an unreflected pump power of 69 mW. The corresponding slope efficiency of 5.8% is in good agreement with the 6% observed under CW operation of a gain element from the same wafer [15]. It is worth noting that the CW experiment used a gain element, that was capillary bonded to a single-crystal diamond heat spreader to enable high-power ( $\sim 1$ W) operation. In a mode-locked laser this additional intra-cavity element can provide undesirable modulation of the gain resulting in pulse stretching. Hence, the diamond heat spreader was not implemented in the present experiment. However, no thermal rollover was observed suggesting that higher output powers could be obtained by using a more powerful pump source.

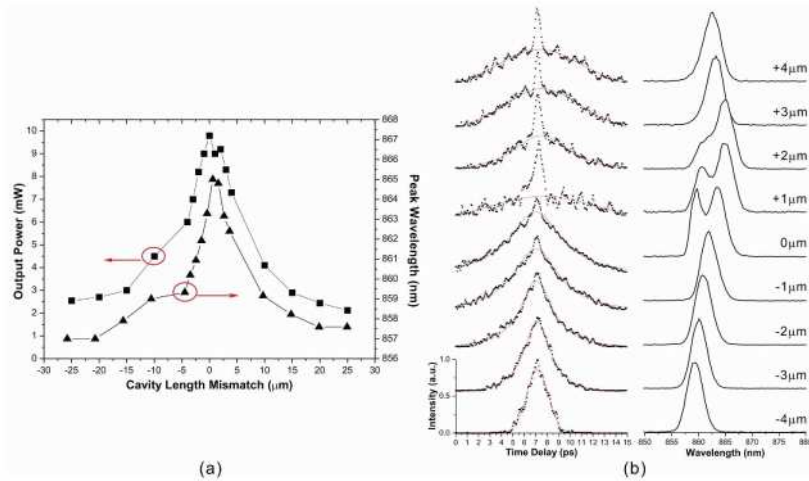


Fig. 2. , VECSEL power and peak wavelength at different cavity lengths (a); autocorrelation traces (dotted curves) and their Lorentzian fits (solid curves) as well as the corresponding spectra of the VECSEL output at different cavity lengths (b).

The characteristics of the VECSEL output at different cavity lengths were also investigated. We refer to the optimal cavity position (mismatch 0) as the cavity length, where the highest net gain is seen by the laser pulse and the maximum average power is obtained. Figure 2(a) shows the VECSEL output power and the peak wavelength as a function of the cavity length mismatch. For both quantities abrupt changes were observed in a narrow region 3  $\mu\text{m}$  either side of the optimum point. At either end of the observed range the peak wavelength of the VECSEL was  $\sim 857$  nm while it increased to 865 nm at a cavity detuning of  $\sim 1$   $\mu\text{m}$ , where the spectrum also broadened to  $\sim 7$  nm. The qualitative behavior of a strong red-shift at maximum output power is similar to what has previously been observed for other synchronously pumped systems [11, 20, 21]. The observed tendency for the peak wavelength vs. mismatch is also confirmed by numerical simulations of a synchronously barrier-pumped VECSEL [14], though we caution that Ref [14]. reports only results for two values of the mismatch. One contributing factor for the wavelength shift might be that the background carrier density during the pulse is higher for the mismatched cavity than for the optimal one because the lower output power indicates that fewer carriers undergo stimulated emission. Due to phase-amplitude coupling described by the line-width enhancement factor [22] this implies that the refractive index is lower, which leads to a blue-shift of the wavelength experiencing resonant periodic gain. In addition, the gain peak is blue-shifted for higher carrier density. Furthermore, chirping might be significant [12]. If the cavity is too short/long, the laser will favor a wavelength travelling slower/faster through the gain medium. As we will

show below, the GVD changes from positive (up-chirp) to negative (down-chirp) across the pulse, which corresponds to a blue-shift in both cases. The widening of the spectrum near the centre of the range coincides with a position where the chirp is expected to be almost linear offering the prospect of short pulses after extra-cavity compression.

The autocorrelation of the laser pulse was also recorded and considerable variations again observed in the  $-4 \mu\text{m}$  to  $+4 \mu\text{m}$  region. The autocorrelation traces and spectra in this detuning range are shown in Fig. 2(b). As the laser cavity was shortened from  $+4 \mu\text{m}$  to  $0 \mu\text{m}$ , the FWHM of the autocorrelation first narrowed from 12 ps to 6.4 ps, then quickly broadened to about 14 ps and finally decreased to 5 ps again. In the positive detuning region, a strong coherent spike was present in the autocorrelation function [11, 21]. From  $0 \mu\text{m}$  to  $-4 \mu\text{m}$ , the autocorrelation width narrowed continuously from 5 ps to 2 ps. Further cavity shortening only resulted in a drop of gain seen by the laser pulse and corresponding reduction in output power.

The spectral bandwidth of the pulses generated around the optimal position was around 7 nm with a time-bandwidth products ranging from 7 to 17.5. Synchronously pumped mode-locked lasers are often observed to display a Lorentzian pulse shape [23] with a theoretical time-bandwidth product of 0.22. Thus, our measurements indicate strong chirping of the pulse. By recording the pulse width after passing the laser output through a 10 cm long glass rod with a dispersion of  $\sim 100 \text{ fs/nm}$  the sign of the chirp was found to be different on the two sides of the position where the spectral bandwidth was broadest ( $+1 \mu\text{m}$ ). The pulse generated with a shorter cavity was up-chirped while it was down-chirped with a longer cavity. This agrees well with the observations for the synchronously barrier pumped VECSELs [9–11] and the qualitative features of this can be understood from the model for the GVD of synchronously pumped VECSELs [12]. For negative cavity detunings the frequency chirp is relatively small and negative (dominated by SPM via optical pumping) resulting in the observed clean spectra with narrow bandwidth. The notable feature of the broad, chirped pulse on the positive displacement side around  $+1 \mu\text{m}$  is caused by the strong chirp near the peak of the gain, where the SPM is most strongly affected by gain saturation.

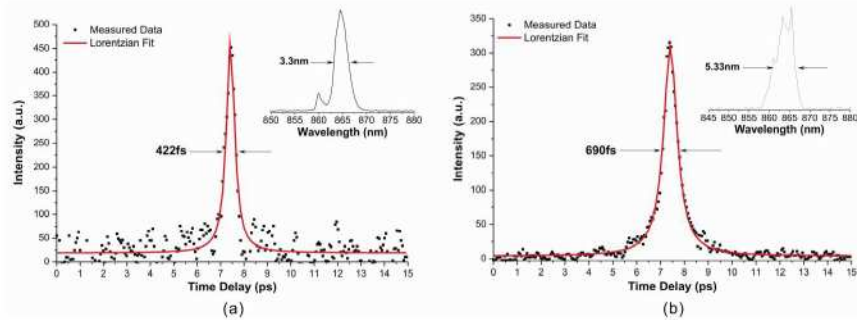


Fig. 3. , Autocorrelation trace of the compressed pulse (a) with a PCF at  $-0.5 \mu\text{m}$  cavity length and (b) with an 8.5 m long telecom fiber at  $+1.5 \mu\text{m}$  cavity length; the insets are the corresponding spectra after the compression fiber.

Extra-cavity dispersion compensation was implemented by using a 2 m long PCF with a zero dispersion wavelength of 810 nm (NL-2.5-810, NKT Photonics A/S) or an 8.5 m long standard telecom fiber. The PCF with a negative GVD of  $70 \text{ ps/km-nm}$  at 860 nm was employed to compensate the positive chirp of the pulse in short cavities. Since PCFs are well known to be highly nonlinear, the nonlinearity induced SPM could potentially result in additional pulse compression [24]. However, no evidence of spectral broadening was observed after the fiber. As shown in Fig. 3(a), effective pulse compression was obtained when the laser cavity was slightly detuned to  $-0.5 \mu\text{m}$ . The best fit to this autocorrelation trace is a Lorentzian pulse shape corresponding to a pulse duration of 210 fs. The spectral bandwidth measured after the PCF was 3.3 nm corresponding to a time-bandwidth product of 0.28, which is close to the Fourier transform limit of 0.22. The average power after the PCF

was about 3.6 mW and the pulse peak power was calculated to be 226 W. Pulse compression by the telecom fiber with a positive GVD of 90 ps/km-nm at 860 nm was successfully achieved for the long cavities. Figure 3(b) shows the compressed pulse at a cavity detuning of +1.5  $\mu\text{m}$ . The laser pulse was compressed from 4.4 ps to 345 fs (Lorentzian pulse-shape assumed). The FWHM spectral width of the pulse after the fiber was measured to be about 5.3 nm resulting in a time-bandwidth product of 0.74 or 3.3 times of the transform limit. The average power out of the fiber was 5.5 mW with a corresponding peak power of 210 W. Compared with the barrier pumped case where a 200 m telecom fiber was employed for chirp compensation [11], the synchronously in-well pumped VECSEL with a comparable pump power only required an 8.5 m telecom fiber for pulse compression. The chirp of the laser pulse for the in-well pumped laser was thus more than one order of magnitude less.

#### 4. Conclusion

We have explored a new concept in ultra-short pulse VECSELs through a combination of synchronously pumped mode-locking and in-well pumping. Due to the elimination of the ~20 ps carrier transportation time in-well pumping leads to faster gain dynamics and correspondingly shorter output pulses from the laser. In this case we observed pulse widths in the range 1 ps to 7 ps directly from the laser, which is approximately an order of magnitude shorter than for a comparable barrier pumped system [11]. Indeed, we observe that an order of magnitude less extra-cavity dispersion is required to compress the laser pulses using either a 2 m long PCF or an 8.5 m standard telecom fiber. After compression, a 210 fs pulse with a peak power of 226 W and a 345 fs pulse with a peak power of 210 W were obtained when the cavity was adjusted to the positions of  $-0.5 \mu\text{m}$  and  $+1.5 \mu\text{m}$ , respectively. A direct comparison between the in-well and barrier-pumped lasers is difficult because the gain material (emission wavelengths) and the wafer structure were different. For a rough analysis one can compare the absorbed pump power of 280 mW (in-well) vs. 450 mW (barrier) [11] which would indicate that the total number of carriers generated was different by roughly a factor of two in the two experiments. Since the pump area for barrier-pumping [11] was also about a factor of two larger than for in-well pumping, the generated carrier density (sheet density integrated longitudinally over the structure) might actually be comparable. Since the amount of chirp should be related to the total carrier density [12], this indicates superior chirp characteristics for in-well pumping, potentially due to the faster gain dynamics. For a detailed assessment numerical simulations and/or a direct experimental comparison with the same samples would be desirable.

The average output power obtained for the results presented here and hence the peak powers are entirely limited by the available pump power and the relatively low absorption of the in-well pumped gain element. Higher pump powers would be expected to result in a higher output power in line with the observations on CW systems [15, 16]. An optimization of the gain element structure for in-well pumping would allow for a further increase. This optimization would include tailoring the system for a more suitable fixed wavelength pump laser, e.g. frequency doubled fiber laser or diode pumped solid state laser, instead of the Ti:Sapphire laser used for the present demonstration.

The reduced chirp of the gain element opens up the additional possibility of femtosecond pulses being generated directly from the laser in conjunction with the intra-cavity dispersion compensation techniques, e.g. chirp mirrors. Combining these improvements would result in a compact, inexpensive high peak-power laser system particularly suitable for e.g. nonlinear, biological imaging applications. The 865 nm output reported here is comparable to what is generally used for multi-photon microscopy [6] while the use of synchronized pump and laser photons provide both sources required for CARS microscopy [7]. The frequency difference between these photons can be controlled by the design of the gain structure and potentially enabling access to the 500-3000  $\text{cm}^{-1}$  range of primary interest for CARS applications.